On the development of a new nonhydrostatic atmospheric model in South Africa

F.A. Engelbrecht[a‡], J.L. McGregor[b] and C.J. deW. Rautenbach[a]

With the advent of ever faster computers, the operational use of nonhydrostatic atmospheric models at resolutions beyond the hydrostatic limit has become a reality. A renewed global research effort is being made to formulate and improve nonhydrostatic models. In this paper, the status of numerical atmospheric modelling research in South Africa is briefly reviewed. We then report on the development of a new, nonhydrostatic atmospheric model at the University of Pretoria. The dynamic kernel of the model is based on a novel, split semi-Lagrangian formulation of a set of quasi-elastic equations in a terrain-following vertical coordinate based on the full pressure field. The main features of the model dynamics and numerics are discussed, and it is noted that the governing equation set presented here has not been applied in atmospheric modelling before. The model may be used to perform state-of-the-art research in numerical model development, for instance, for the derivation of new equation sets, numerical techniques and vertical coordinate systems. The model's ability to simulate highly nonlinear and nonhydrostatic flow is illustrated by means of a convective bubble experiment, where an updraft interacts with vertical shear of the horizontal wind. This experiment illustrates the potential of the new model to be used in the study of thunderstorm dynamics.

Introduction

The single most fundamental simplification that may be introduced to the fully-elastic atmospheric equations is probably the 'hydrostatic approximation'. Having its roots in a scale analysis of synoptic-scale systems,[1] the approximation consists of neglecting the vertical acceleration term in the vertical momentum equation. It thereby assumes a perfect force balance in the vertical, between gravity and the vertical pressure gradient force. The resolution of operational numerical weather prediction (NWP) models has until fairly recently been limited by computing power and operational time constraints to resolutions where the hydrostatic approximation is almost perfectly valid. Operational forecasts therefore have mostly relied on hydrostatic models. However, the development of nonhydrostatic atmospheric models (which retain the vertical acceleration term) has been pursued for more than four decades, beginning with different mesoscale investigations.[2–7] With computer systems becoming faster and more affordable over the past decade, there has been a corresponding increase in the spatial resolution of both NWP and climate simulation models. This has encouraged the transition of the highly developed hydrostatic models to nonhydrostatic models. Over the past decade, atmospheric research institutions have started to replace operational hydrostatic models with nonhydrostatic versions.[8–10] Model upgrading is much easier if connections with the existing hydrostatic model are preserved during the development of the nonhydrostatic alternative.[11] In this regard, preserving the vertical coordinate of the hydrostatic model (usually some type of pressure coordinate) is highly desirable.

Using the fastest supercomputers available, global simulations at resolutions of about 10 km in the horizontal (in the region of the hydrostatic limit) have recently been performed.[12,13] It is interesting to note that these simulations were carried out with hydrostatic models, although nonhydrostatic versions are under development.[13] An important conclusion from these experiments is that a better understanding of the role of physical parameterizations in models is essential to obtain full benefit of the potential increase in accuracy provided by such high spatial resolution.[13] Over relatively small domains, operational model resolutions are already beyond the hydrostatic limit. That is, these models run at resolutions higher than 10 km, where convection is at least partially resolved (i.e. partially explicitly simulated) by nonhydrostatic models. Convection can probably be fully resolved only at model resolutions of about two orders of magnitude higher, that is, about 100 m in the horizontal. It is therefore likely that, for many years to come, operational nonhydrostatic models will function at resolutions where convection can be only partially resolved.

The use of convection parameterization schemes at these resolutions is a relatively unexplored field of study in atmospheric modelling. The parameterization schemes applied in hydrostatic models have generally been designed to function at resolutions where convection cannot be resolved at all. These schemes need to be reviewed and probably modified to function properly beyond the hydrostatic limit. Theoretical research on the explicit simulation of moist convection is another growing field of study, and nonhydrostatic models are a primary tool for these investigations. Explicit simulations of moist convection will benefit the design of convection parameterization schemes for application at model resolutions where convection cannot be fully resolved.

Against this background of renewed interest in the improvement of nonhydrostatic models and the explicit simulation of convection, this paper reports on the development of a new nonhydrostatic model in South Africa. We begin with a brief overview of the status of numerical atmospheric modelling in the country. The dynamic equations and distinctive properties of the numerical formulation of the new model are then discussed. The ability of the model to simulate highly nonlinear and nonhydrostatic flow is illustrated by means of a convective bubble experiment. Finally, some conclusions are drawn and potential applications of the new model are indicated.

Numerical atmospheric modelling in South Africa

In the 1960s, a small group of scientists from the Council for Scientific and Industrial Research (CSIR) and the South African Weather Bureau (SAWB) became the first South Africans to develop a NWP model.[14] The group was headed by A.P. Burger of the CSIR. The first to be developed was a quasi-geostrophic barotropic model, which was applied over the southern hemisphere at the 500-hPa level.[15] Theoretical investigations by Riphagen and Burger led to the development of the first multi-level model applied in South Africa, a new filtered quasi-

[a]Department of Geography, Geoinformatics and Meteorology, University of Pretoria, Pretoria 0002, South Africa.
[b]CSIRO Marine and Atmospheric Research, PB1 Aspendale, 3195, Victoria, Australia.
‡Author for correspondence. E-mail: francois.engelbrecht@up.ac.za

geostrophic model based on energy conservation principles.[16–18] When this model was first used operationally in the 1970s, it was integrated over only two or three levels in the vertical because of computational constraints (H.A. Riphagen, pers. comm.). The model ran operationally at the SAWB, as a backup for a hydrostatic primitive equation model obtained from abroad.

In the early 1980s, a five-level, split-explicit, hydrostatic primitive equation model for hemispheric prediction (with a nesting option) was developed at the CSIR.[19] Its performance was evaluated over an 18-month semi-operational period at the SAWB, and it was found to be comparable to that of the international model used at the time. A theoretical investigation of the computational stability of the model was carried out, which resulted in a longer time step being allowed.[20] The introduction of a semi-Lagrangian advection scheme further enhanced the model's efficiency.[21]

The work on the hydrostatic primitive equation model by Riphagen[19–22] provided an excellent foundation for future model development in South Africa. Unfortunately, policy changes at the CSIR in the mid-1980s caused the organization to become more commercially driven, and research into NWP became a low priority. Riphagen joined the SAWB in 1986. Here, however, it was policy to obtain model codes from abroad, rather than to maintain and improve a locally developed code.

Since most meteorologists in South Africa were employed by the SAWB [and today by the South African Weather Service (SAWS)], only a few further studies in the field of numerical meteorology were conducted here.

These were mostly concerned with modifying the vertical coordinate system of the international Eta model[23–25] and with data assimilation systems applied in some of the the international models that became operational at the SAWB.[26] At the University of Pretoria (UP), a hybrid sigma-pressure vertical coordinate was introduced in the dynamic formulation of an atmospheric general circulation model (AGCM).[27] Generally, there has been a progressive decline in research activities related to numerical atmospheric modelling in South Africa over the last two decades. Today, therefore, the country lacks meteorologists skilled in the field of numerical atmospheric modelling.

It may be noted that Burger and Riphagen wrote significant papers on how to obtain energy-consistent approximations of the atmospheric equations.[28–30] In a study of the equations of motion expressed in an arbitrary vertical coordinate system, they[29] retain in the components of the momentum equation the Coriolis terms that vary with the cosine of the latitude (the $\cos\rho$ terms) and other terms not included in the hydrostatic primitive equations.[31] The omission of the $\cos\rho$ terms has been called the traditional approximation.[32] The paper by Burger and Riphagen[29] preceded a recent international trend in global atmospheric modelling, in which the hydrostatic primitive equations (that contain the traditional approximation) are replaced by more complete quasi-hydrostatic[33] or fully elastic nonhydrostatic[10,34] equation sets that contain a representation of the full Coriolis force.

Although local model development ceased in the mid-1980s in South Africa, a wide range of internationally developed numerical models have been applied in the country. Since 1992, the Eta model from the National Centers for Environmental Prediction (NCEP) has been the base model to obtain daily weather forecasts issued by the SAWB (and subsequently by SAWS). The Eta model has also been used in case studies of severe thunderstorms over South Africa.[35,36] The SAWS is currently in the process of replacing the Eta model with the United Kingdom Meteorological Office (UKMO) regional forecast model (W.J. Tennant, pers. comm.). The European Center-Hamburg model version 4.5 (ECHAM4.5) AGCM also runs in-house at the weather service in order to provide seasonal forecasts.[37]

Some universities in South Africa have also managed to implement international models locally. At the University of the Witwatersrand (Wits), sensitivity experiments with the Regional Atmospheric Modelling System (RAMS) were performed in the 1980s and 1990s.[38,39] The regional climate model DARLAM (Division of Atmospheric Research Limited Area Model) was also applied to perform climate simulations over southern Africa.[40] Since then, the climatology group at Wits has found different focus areas. The University of Cape Town (UCT) has become more active in the field, and has been performing climate simulations with the Fifth Generation Pennsylvania State University-National Center for Atmospheric Research (NCAR) Meso-scale Model (MM5) since the 1990s. Recently, ten-year MM5 simulations of present and future climate over southern Africa were performed and described.[41] Studies of interannual climate variability including sensitivity to SSTs have been performed using MM5 and the global Hadley Centre Atmospheric Model Version 3 (HadAM3) at UCT,[42,43] while the dynamics of a heavy rainfall event have also been studied using MM5.[44] At the University of Pretoria, the CSIRO Mark II atmospheric general circulation model has been used in sensitivity studies to explore ocean surface and atmosphere interaction[45–47] and for seasonal forecasting.[48] Simulations of climate and climate change over southern and tropical Africa have also been performed at UP, using the CSIRO's DARLAM and the Conformal-Cubic Atmospheric Model (CCAM).[49,50]

Intensive research on atmospheric model development began at the University of Pretoria in 2002, as part of a project sponsored by the South African Water Research Commission (WRC). During the course of the project, the hydrostatic CCAM was implemented on the university's computers. Various sensitivity studies were performed to improve the model's ability to simulate rainfall over southern Africa.[51] With the assistance of CSIRO scientists, the research group at UP managed to operate CCAM for routine NWP over southern Africa.[51] UP is the first institution in South Africa, other than the SAWS, to accomplish this. An important aspect of the WRC project was the development of a nonhydrostatic kernel for a new atmospheric model,[52] which contributed to the creation of a nonhydrostatic kernel for CCAM.

Governing equations and numerical formulation

The new numerical model employs the terrain-following σ coordinate equivalent of the anelastic nonhydrostatic pressure coordinate equations of White.[53] These equation sets are based on the full pressure field, and the σ coordinate is defined as

$$\sigma = \frac{p - p_T}{p_{surf} - p_T} = \frac{p - p_T}{p_s}. \tag{1}$$

Here p represents the full pressure field, p_T is the prescribed pressure at the model top (a constant), p_{surf} is the full surface pressure, and $p_s = p_{surf} - p_T$. The set of nonhydrostatic equations given by White[53] may be transformed from the pressure coordinate into the σ coordinate to give the following set of momentum, continuity and thermodynamic equations:[52]

$$\frac{Du}{Dt} - fv + \frac{\partial\phi}{\partial x} - \sigma\frac{\partial\phi}{\partial\sigma}\frac{\partial \ln p_s}{\partial x} = 0, \tag{2}$$

$$\frac{Dv}{Dt} + fu + \frac{\partial\phi}{\partial y} - \sigma\frac{\partial\phi}{\partial\sigma}\frac{\partial \ln p_s}{\partial y} = 0, \tag{3}$$

$$\frac{R}{g}\frac{D}{Dt}\left(\frac{\omega T}{p}\right) + g + \frac{p}{p_s}\frac{g}{RT}\frac{\partial\phi}{\partial\sigma} = 0, \tag{4}$$

$$\frac{\partial u}{\partial x}+\frac{\partial v}{\partial y}+\frac{\partial \dot{\sigma}}{\partial \sigma}+\frac{D\ln p_s}{Dt}=0, \tag{5}$$

$$\frac{DT}{Dt}-\kappa\frac{\omega T}{p}=0. \tag{6}$$

In Equations (2) to (6) the material derivative is defined as

$$\frac{D}{Dt}=\frac{\partial}{\partial t}+u\frac{\partial}{\partial x}+v\frac{\partial}{\partial y}+\dot{\sigma}\frac{\partial}{\partial \sigma}. \tag{7}$$

Equations (2) to (6) describe a dry, adiabatic atmosphere without friction; x and y are horizontal Cartesian coordinates and t is time. All differentiations with respect to time and the horizontal coordinates are carried out at constant σ. The components of the horizontal wind are u and v; ϕ is the geopotential, gz, z being geometric height; T is temperature, $\dot{\sigma}=D\sigma/Dt$ and $\omega=Dp/Dt$. R is the gas constant for dry air and $\kappa=R/c_p$, with c_p the specific heat of dry air at constant pressure; f is the Coriolis parameter. It is convenient to introduce the variable Ω by noting the relation between the fields $\dot{\sigma}$ and ω:

$$\Omega=\frac{\omega}{p}=\frac{p_s}{\sigma p_s+p_T}\left(\sigma\frac{D\ln p_s}{Dt}+\dot{\sigma}\right). \tag{8}$$

Equations (2) to (6) with (8) may be combined to give an elliptic equation for the geopotential,[52]

$$\begin{aligned}
&\frac{\partial^2\phi}{\partial x^2}+\frac{\partial^2\phi}{\partial y^2}+\frac{\partial}{\partial\sigma}\left(s^2\frac{\partial\phi}{\partial\sigma}\right)-2\sigma\left(\frac{\partial\ln p_s}{\partial x}\frac{\partial^2\phi}{\partial x\partial\sigma}+\frac{\partial\ln p_s}{\partial y}\frac{\partial^2\phi}{\partial y\partial\sigma}\right)+\\
&\left[\left(\frac{\partial\ln p_s}{\partial x}\right)^2+\left(\frac{\partial\ln p_s}{\partial y}\right)^2\right]\left[\frac{\partial}{\partial\sigma}\left(\sigma^2\frac{\partial\phi}{\partial\sigma}\right)\right]-\frac{\sigma}{p_s}\left(\frac{\partial^2 p_s}{\partial x^2}+\frac{\partial^2 p_s}{\partial y^2}\right)\frac{\partial\phi}{\partial\sigma}=\\
&2\left\{\left(\frac{\partial u}{\partial x}+\frac{\partial v}{\partial y}\right)\frac{\partial}{\partial\sigma}\left(\Omega\frac{p}{p_s}\right)\right.\\
&-\frac{1}{p_s}\left[\frac{\partial}{\partial x}(\Omega p)\frac{\partial u}{\partial\sigma}+\frac{\partial}{\partial y}(\Omega p)\frac{\partial v}{\partial\sigma}\right]+\frac{\partial u}{\partial x}\frac{\partial v}{\partial y}-\frac{\partial v}{\partial x}\frac{\partial u}{\partial y}+\\
&\left.\sigma\left[\frac{\partial\ln p_s}{\partial x}\left(\frac{\partial u}{\partial y}\frac{\partial v}{\partial\sigma}-\frac{\partial v}{\partial y}\frac{\partial u}{\partial\sigma}\right)+\frac{\partial\ln p_s}{\partial y}\left(\frac{\partial v}{\partial x}\frac{\partial u}{\partial\sigma}-\frac{\partial u}{\partial x}\frac{\partial v}{\partial\sigma}\right)\right]\right\}\\
&+f\left[\frac{\partial v}{\partial x}-\frac{\partial u}{\partial y}+\sigma\left(\frac{\partial u}{\partial\sigma}\frac{\partial\ln p_s}{\partial y}-\frac{\partial v}{\partial\sigma}\frac{\partial\ln p_s}{\partial x}\right)\right]\\
&-u\frac{df}{dy}-\frac{\partial}{\partial\sigma}\left(sg-\frac{p}{p_s}\Omega^2\frac{1}{\gamma}\right).
\end{aligned} \tag{9}$$

Here, $s=(\sigma+p_T/p_s)(g/RT)=(p/p_s)(g/RT)$ and $\gamma=c_p/c_v$, with c_v the specific heat of dry air at constant volume. Equation (9) is needed during the numerical solution of governing Equations (2) to (6).[52]

Note that (2) to (6) and (9), corresponding to the pressure coordinate equations of White,[53] are formulated independently of the use of a reference thermodynamic profile. This facilitates the application of the model at spatial scales larger than the meso-scale.[53] In the pressure coordinate formulation,[53] vertically propagating sound waves are absent. Lamb waves may be filtered by applying the lower boundary condition $\omega=0$ at $p=p_0$, with p_0 a constant.[53,54] Thus, the pressure coordinate equation set is anelastic. Equations (2) to (6) may also be shown to be filtered of vertically propagating sound waves, but horizontally propagating sound waves (Lamb waves) are present.[52,54] This renders the σ coordinate equations quasi-elastic, and implies a computational penalty with respect to the corresponding pressure coordinate equations.[54] However, it is well known that, generally, the lower boundary $\dot{\sigma}=0$ at $\sigma=1$ offers significant advantages over an equivalent pressure coordinate formulation.[55] It may also be noted that the filtering of the vertically propagating sound waves in Equations (2) to (6) implies a computational advantage over the fully-elastic equations. The buoyancy modes described by Equations (2) to (6) are largely undistorted from the unapproximated equation form.[52,54–56] It may be noted that the use of the σ coordinate based on the full pressure field is in contrast to the recent trend of formulating fully-elastic nonhydrostatic models in terms of a vertical coordinate based on the hydrostatic pressure field.[8,9,11,57–59] Existing hydrostatic σ coordinate models may be converted with relative ease to nonhydrostatic models based on the quasi-elastic σ coordinate equations.[52]

A novel time-split semi-Lagrangian scheme has been formulated to solve the quasi-elastic equations efficiently on a non-staggered grid.[52] The solution procedure involves the splitting of the terms in Equations (2) to (6) into advective and non-advective terms. The equations may then be solved in four phases. In the first phase, the advective terms are discretized with a semi-Lagrangian procedure having a time step Δt_s. This is followed by the application of explicit diffusion to the horizontal wind and temperature fields. In the third phase, the non-advective terms are treated in an adjustment procedure having N time steps of size $\Delta t_a=\Delta t_s/N$. In the final phase, a highly scale-dependent spatial filter is applied to the velocity, surface pressure and geopotential fields in order to remove two-grid-interval waves[60] from the non-staggered grid. The distinctive features of the numerical model are:[52]

- nonhydrostatic, quasi-elastic formulation using a terrain-following coordinate based on the full pressure field;
- two time-level, time-split time integration scheme involving an advection, diffusion, adjustment and spatial filtering step;
- spatial discretization on a grid that is non-staggered in both the horizontal and vertical;
- semi-Lagrangian advection for the horizontal wind, surface pressure and temperature, using McGregor's[61] method for the calculation of departure points. Tri-cubic spatial interpolation is used to evaluate the values of variables at the departure points;
- forward-backward time differencing in the adjustment phase;
- fourth-order accurate centred spatial differencing on the non-staggered grid;
- high-order, highly scale-dependent Shapiro[62] spatial filtering;
- option of explicit diffusion available;
- consistent evaluation of the surface pressure and vertical motion field by using the continuity equation;
- semi-implicit treatment of the Coriolis terms;[63,64]
- three-dimensional iterative solution of a variable-coefficient, non-linear elliptic equation for the geopotential at each adjustment time-step, using successive over-relaxation.

It may be noted that the stability and accuracy properties of the split semi-Lagrangian scheme have been studied by means of a series of bubble convection tests.[52] The model produced solutions that compare well with results obtained by other authors who have performed the same tests using fully-elastic numerical models.[9,11,65,66] The scheme is stable at large Courant numbers, provided that the Shapiro[62] filter is applied regularly to remove two-grid-interval noise from the non-staggered grid. The new model has been named the 'Nonhydrostatic Sigma-coordinate Model (NSM)'.[52]

A simulation of highly nonlinear and nonhydrostatic flow

Design of the experiment

In this three-dimensional experiment, a warm disturbance in the potential temperature is introduced to an atmosphere with strong unidirectional vertical wind shear. The initial environment

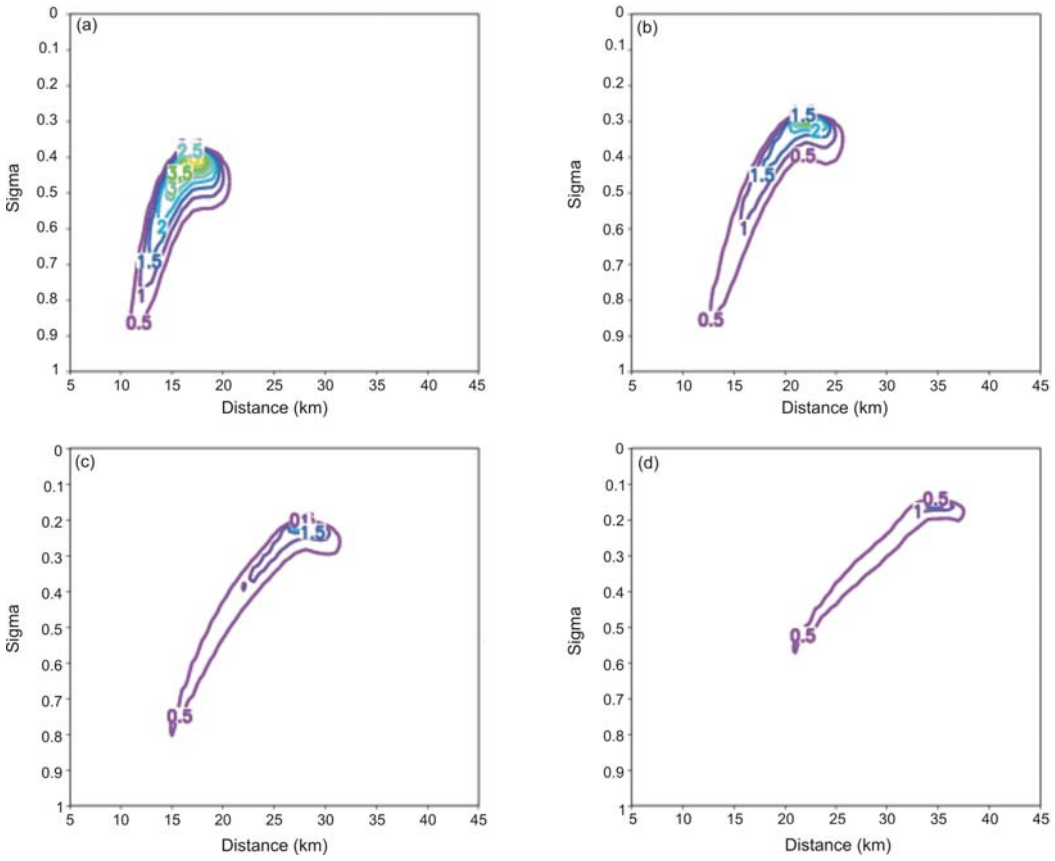

Fig. 1. A three-dimensional warm bubble rising in an environment with strong unidirectional vertical wind shear. Vertical cross section of the potential temperature perturbation at y = 25 000 m and $0 \le \sigma \le 1$; (**a**) after 360 s, (**b**) after 540 s, (**c**) after 720 s, (**d**) after 900 s. The contour interval is 0.5 K.

is dry, isentropic with potential temperature 300 K, and in hydrostatic balance. The x component of the initial horizontal wind has vertical shear

$$\frac{du}{dz} = 0.005 \text{ s}^{-1}, \tag{10}$$

that is, the x component of the horizontal wind increases by 20 m s^{-1} over each interval of 4000 m in the vertical. The initial y components of the horizontal wind and vertical motion field are zero. It may be noted that wind shear values of 0.003–0.005 s^{-1} are associated with the formation of supercell (rotating) thunderstorms.[67–69] The wind shear value in the experiment falls in this category. Although unidirectional wind shear occurs rather infrequently in the atmosphere,[70] the development of rotation in thunderstorms and the occurrence of storm-splitting have been observed in environments with unidirectional vertical wind shear of sufficient magnitude.[71]

The integration domain extends over $0 \le x \le 50\,000$ m and $0 \le y \le 50\,000$ m in the horizontal. The top of the model domain is chosen to be 135 hPa (about 13 500 m). The shape and intensity of the initial disturbance in the potential temperature is given by

$$\Delta\theta_0(x, y, z) = 6.6\cos^2(\frac{\pi}{2}r), \tag{11}$$

for $r \le 1$, where $r^2 = [(x - x_c)/x_t]^2 + [(y - y_c)/y_t]^2 + [(z - z_c)/z_t]^2$, x_c = 10 000 m, y_c = 25 000 m, z_c = 2750 m, and $x_t = y_t = z_t$ = 2500 m.

In its initial position, the centre of the bubble is located 10 000 m away from the upstream boundary x = 0 m. The horizontal resolution used is 1000 m, and 135 equally spaced σ levels are used to give a vertical spacing of about 100 m on the average.

For the bubble convection tests, the model employs free-slip vertical boundary conditions. At the lateral boundaries, $\dot{\sigma} = 0$ and the horizontal gradient of v is assumed to vanish. The u field is kept constant at its initial vertical profile determined by (10) during the integration period, at all the lateral boundaries. The model employs an initialization procedure that exploits the elliptic Equation (9).[52] The split semi-Lagrangian scheme[52] is used to solve the governing quasi-elastic σ coordinate equations presented in the paper. For this particular experiment, explicit horizontal diffusion is applied to the horizontal wind components and the temperature field, with the explicit diffusion coefficients chosen to be K_s = 300 m^2 s^{-1} and K_{Ts} = 50 m^2 s^{-1}.[52] Diffusion of similar magnitudes is applied along the σ axis, for u and T, respectively. These values of the diffusion coefficients are similar to those used in typical two-dimensional warm bubble experiments.[11,52] The use of explicit diffusion contributes to controlling two-grid-interval waves on the non-staggered grid.[52] Being of no relevance to the study of bubble convection, the Coriolis effect is neglected in the experiment. The advection and adjustment time steps used are Δt_s = 1.2 s and Δt_a = 0.3 s, respectively, and the integration period is 900 s.

Horizontal splitting of the disturbance in the environment with vertical wind shear

The potential temperature perturbation θ' from the isentropic background state after 360, 540, 720 and 900 s is shown in Fig. 1, for a vertical cross section along y = 25 000 m. The contour interval is 0.5 K. The corresponding vertical velocity fields w are shown in Fig. 2, with the contour interval 1 m s^{-1}. Horizontal cross sections of θ' at levels of constant σ are shown in Fig. 3, for t = 360, 540, 720 and 900 s. The contour interval is 0.5 K. The constant sigma levels are 0.44, 0.37, 0.29 and 0.22 for panels (a)–(d) of Fig. 3, respectively. For each of the time-levels, the σ level used corresponds to the height at which the vertical velocity attains a maximum along y = 25 000 m. Note the displacement of

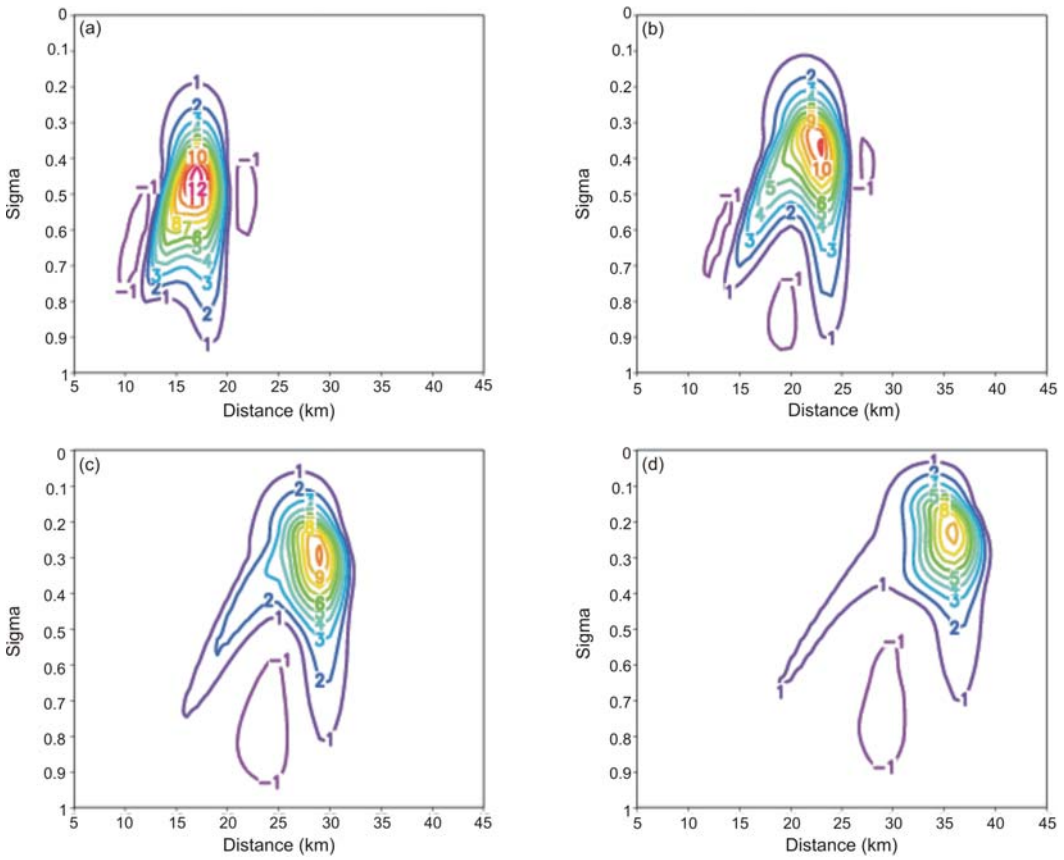

Fig. 2. As for Fig. 1 but showing the vertical cross section of the vertical component of the wind w at $y = 25\,000$ m and $0 \leq \sigma \leq 1$: (**a**) after 360 s, (**b**) after 540 s, (**c**) after 720 s, (**d**) after 900 s. The contour interval is 1 m s^{-1}. Note the formation of a rotor-like circulation around the initial updraft, as is indicated by regions of negative vertical velocity in panels (a) and (b).

the portion of the horizontal domain shown in Fig. 3(a)–(d).

Figure 1 shows how the warm bubble rises in the environment with strong vertical wind shear, while being advected in the positive x direction by the u component of the wind. The strongest vertical wind speed simulated is about 12 m s^{-1}, which is typical of an updraft in a small convective cell in the mid-latitudes. Because of the increase in the magnitude of u with height, the horizontal displacement of the upper part of the bubble takes place the fastest. Initially, the updraft induced by the positive buoyancy of the bubble is tilted slightly in the positive x direction by the horizontal wind field (Fig. 2a). Rotors develop along the outermost edges of the bubble (note the downdrafts in Figs 2a and 2b). These rotors are even better developed along the flanks of the bubble that are perpendicular to the advecting wind u (not shown). With time, the core of the updraft gradually changes its orientation and eventually it is tilted in the negative x direction (Figs 2c and 2d).

Figure 3 shows how the potential temperature perturbation maximum on the σ level that corresponds to the height of maximum vertical velocity, splits around the vertical centre axis of the bubble during its displacement in the positive x direction by the horizontal wind. Two potential temperature maxima, one on each side of the vertical centre axis, are well developed by $t =$ 900 s. The 'horizontal splitting' of the potential temperature disturbance is indicative of a feature that is well-known from the linear theory of rotating thunderstorms, namely 'storm splitting'.[1,70,72] In an environment characterized by strong unidirectional vertical wind shear, low pressure areas develop on both the left and right flanks of the original updraft.[73] These tend to be the strongest at the middle levels of the atmosphere. The associated pressure forcing may be sufficient to cause the updraft to split into two separate updrafts moving to the left and right of the environmental wind. The left- and right-moving updrafts rotate clockwise and anticlockwise, respectively. The rotation that develops is the result of the tilting of horizontal shear vorticity into the vertical by the original updraft.[1,73,74] Storm splitting has indeed been observed for cases where strong unidirectional wind shear occurred in the real atmosphere.[71]

Figure 4 shows the vertical velocity w (shaded) and the vertical component of the vorticity $\zeta = \partial v/\partial x - \partial u/\partial y$ (contours) at $t =$ 900 s, for a portion of the horizontal domain at $\sigma = 0.48$. Indeed, negative vorticity (indicating clockwise rotation) and positive vorticity (indicating anticlockwise rotation) are present to the left and right of the centre axis $y = 25\,000$ m, respectively. The development of the potential temperature maxima on each side of this centre axis (Fig. 3d) may be attributed to advection that results from the two counter-rotating vortices. Two well-established updrafts can also be seen at $t = 900$ s (Fig. 4), moving to the left and right of the environmental wind. It is interesting to note that a single updraft still exists at $t = 900$ s at the $\sigma =$ 0.22 level (not shown) of maximum vertical velocity (Fig. 2d), and that the splitting of the original updraft into two separate updrafts is most noticeable well below that level.

The results described in this section qualitatively resemble the linear theory of storm splitting and the development of rotation in thunderstorms.[1] Clearly, the new model kernel based on a split semi-Lagrangian formulation of the quasi-elastic equations can be used adequately to describe highly nonlinear and non-hydrostatic flow. A detailed study of the dynamics relevant to the present experiment falls beyond the scope of this paper, but the experiment illustrates the potential of NSM to be used in the study of nonhydrostatic circulation systems.

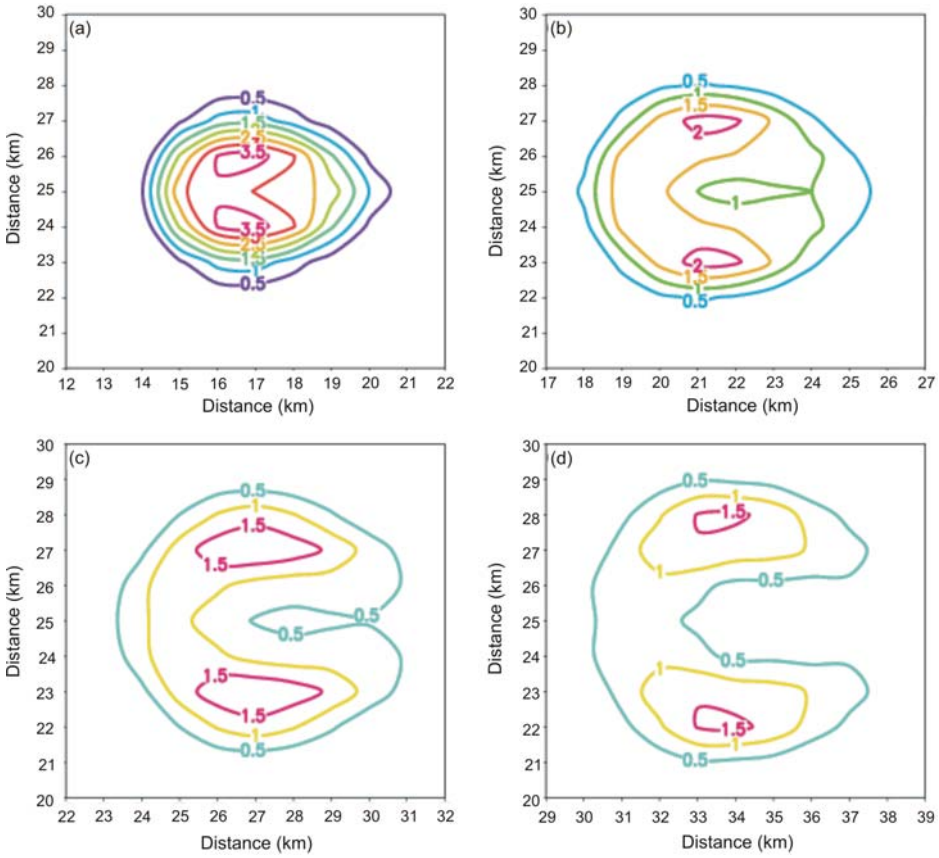

Fig. 3. As for Fig. 2 but showing the horizontal cross section of the potential temperature perturbation. (**a**) after 360 s at $\sigma = 0.44$, (**b**) after 540 s at $\sigma = 0.37$, (**c**) after 720 s at $\sigma = 0.29$, (**d**) after 900 s at $\sigma = 0.22$. The contour interval is 0.5 K. The σ level used for each time step corresponds to the height of maximum vertical velocity along $y = 25\,000$ m. Note that only the region $20\,000 \leq y \leq 30\,000$ m is shown and that there is a displacement of the portion of the x direction domain shown in the panels. The splitting that occurs in the potential temperature field in the environment with vertical wind shear corresponds to the linear theory of 'storm splitting'.

Discussion and conclusions

A new nonhydrostatic atmospheric model has been developed at the University of Pretoria. The dynamic kernel of the model is based on a split semi-Lagrangian formulation[52] of the set of quasi-elastic σ coordinate equations presented in this paper. The equations are the σ coordinate equivalent of the anelastic pressure coordinate equations of White,[53] which are based on the full pressure field. The σ coordinate equations contain Lamb waves as part of the solution set, but vertically propagating sound waves have been filtered out. Thus, the new model is quasi-elastic, and offers a computational efficiency advantage over nonhydrostatic models based on the fully-elastic equations.[52] The model equations are formulated independently of the use of a thermodynamic reference profile, and the model has the potential to be applied also at spatial scales larger than the meso-scale.[53] Existing hydrostatic σ coordinate models may be converted to nonhydrostatic models based on the quasi-elastic σ coordinate equations with relative ease.[52]

The new model's ability to simulate highly nonlinear and nonhydrostatic flow is illustrated by a convective bubble experiment, in which a warm bubble rises in an environment with strong vertical wind shear. The rising bubble is simulated to split in the horizontal plane, with opposite rotating vortices developing on opposite sides of the initial updraft. This result corresponds qualitatively to the linear theory of storm splitting,[1,7,72] and illustrates the usefulness of the new model in studying thunderstorm dynamics. In particular, in further developments we plan to use the model to study the interaction of updrafts with vertical shear of the horizontal wind, convective storm splitting, the development of meso-cyclones in supercell storms, and the merging of cumulus cells and roll convection. The accuracy and stability properties of the split semi-Lagrangian scheme have been tested extensively by a series of bubble convection tests in two and three spatial dimensions.[52] The new scheme is

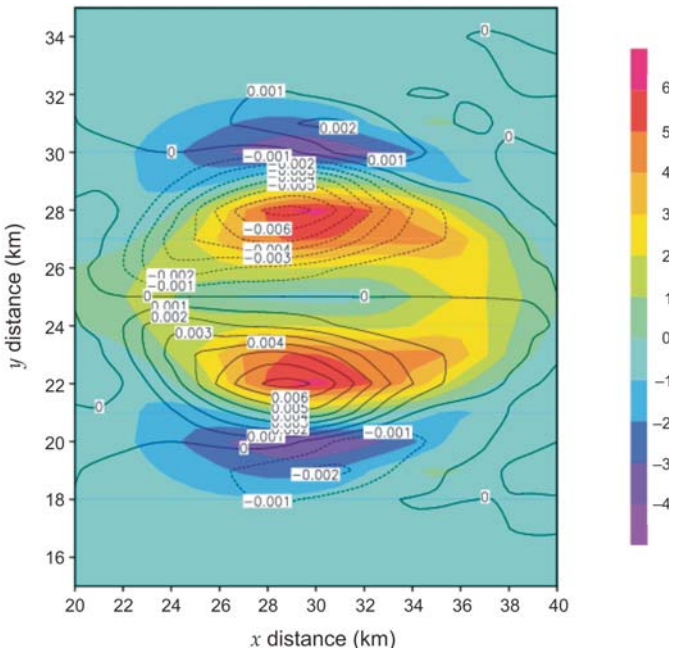

Fig. 4. The vertical component of the wind w (shaded, m s^{-1}) and the vertical component of the vorticity ζ (contours, s^{-1}) at $\sigma = 0.48$ and $t = 900$ s. Note that two counter-rotating vortices have developed on opposite sides of the initial updraft, with new updraft cores centred on each of the vortices.

stable at large Courant numbers and functions well on the non-staggered grid, provided that the Shapiro[62] spatial filter is applied regularly.[52]

Prior to the work reported in this paper, research on a locally developed numerical atmospheric model was dormant in South Africa for about two decades. Local researchers may now contribute more easily to international model development, by benefiting from the capacity that has been developed around the new code. The authors intend to use the new model to contribute to four important, interlinked and growing fields in numerical atmospheric modelling:

- the development of nonhydrostatic models in general (equation sets, vertical coordinates, numerical solution procedures);
- conversion of existing (mostly pressure-based) hydrostatic models into nonhydrostatic versions;
- the study of moist convection by means of explicit numerical simulations performed at spatial resolutions where the convection is adequately resolved;
- the development of convection parameterization schemes for nonhydrostatic models that are applied at resolutions where convection is only partially resolved.

Except for theoretical studies of convective storm features, we intend to use NSM specifically to study the properties of nonhydrostatic circulation systems over South Africa. The dynamics of severe thunderstorms occurring over the country, in particular, are relatively unexplored. The dynamics of mountain waves over the Drakensberg, the Western Cape mountains and Marion Island may also be investigated by using NSM. Furthermore, the model has the potential to produce high-resolution wind simulations that may be used in air pollution dispersion studies, for example over the highveld region of South Africa.

We thank J.D. Gertenbach, H.A. Riphagen and C.J. Potgieter for insightful comments made during the course of the study. G.W. Reuter and M.J. Reeder helped to improve the paper. We also benefited from the comments of two reviewers. The research formed part of the Ph.D. studies of the first author, and contributed to a project on atmospheric model development sponsored by the Water Research Commission (WRC) in South Africa. The support and encouragement of G. Green from the WRC is gratefully acknowledged.

Received 11 August 2006. Accepted 25 January 2007.

1. Holton J.R. (1992). *An Introduction to Dynamic Meteorology,* 3rd edn. Academic Press, San Diego.
2. Ogura Y. and Charney J.C. (1962). A numerical model of thermal convection in the atmosphere. In *Proc. Int. Symp. Numerical Weather Prediction, Tokyo,* pp. 431–451. Meteorological Society of Japan, Tokyo.
3. Dutton J.A. and Fichtl G.H. (1969). Approximate equations of motion for gases and liquids. *J. Atmos. Sci.* **26**, 241–254.
4. Miller M.J. and Pearce R.P. (1974). A three-dimensional primitive equation model of cumulonimbus convection. *Q. J. R. Met. Soc.* **100**, 133–154.
5. Tapp M.C. and White P.W. (1976). A nonhydrostatic mesoscale model. *Q. J. R. Met. Soc.* **102**, 277–296.
6. Klemp J.B. and Wilhelmson R.B. (1978). Simulations of three-dimensional convective storm-dynamics. *J. Atmos. Sci.* **35**, 1070–1096.
7. Pielke R.A. (1984). *Mesoscale Meteorological Modeling.* Academic Press, San Diego.
8. Bubnova R., Hello G., Benard P. and Geleyn J.F. (1995). Integration of the fully elastic equations cast in the hydrostatic pressure terrain-following coordinate in the framework of the ARPEGE/Aladin NWP system. *Mon. Weath. Rev.* **123**, 515–535.
9. Gallus W.A. Jr and Rancic M. (1996). A nonhydrostatic version of NMC's regional Eta model. *Q. J. R. Met. Soc.* **122**, 495–513.
10. Davies T., Cullen M.J.P., Malcolm A.J., Mawson M.H., Staniforth A., White A.A. and Wood N. (2005). A new dynamical core for the Met Office's global and regional modelling of the atmosphere. *Q. J. R. Met. Soc.* **131**, 1759–1782.
11. Janjic Z.I., Gerrity J.P. Jr. and Nickovic S. (2001). An alternative approach to nonhydrostatic modeling. *Mon. Weath. Rev.* **129**, 1164–1178.
12. Ohfuchi W., Sasaki H., Masumoto Y. and Nakamura H. (2005). Mesoscale resolving simulations of the global atmosphere and ocean on the Earth Simulator. *EOS Trans. AGU* **86**, 45–46.
13. Shen B-W., Atlas R., Chern J-D., Reale O., Lin S-J., Lee T and Chang J. (2006). The 0.125 degree finite-volume general circulation model on the NASA Columbia supercomputer: preliminary simulations of mesoscale vortices. *Geophys. Res. Lett.* **33**, L05801, doi:10.1029/2005GL024594.
14. Triegaardt D.O. (1965). The application of dynamic methods of weather prediction to the South African forecasting problem: a progress report. *South African Weather Bureau News Letter,* No. 201, 187–188.
15. Triegaardt D.O. (1965). Experimental barotropic forecasting over subtropical regions. *Notos* **14**, 3–15.
16. Burger A.P. and Riphagen H.A. (1978). *Analysis of energy-consistency of simple weather prediction models.* CSIR Special Report, SWISK 1, Pretoria.
17. Burger A.P. and Riphagen H.A. (1979). The lower boundary condition and energy consistency in primitive and filtered models. *J. Atmos. Sci.* **36**, 1436–1449.
18. Riphagen H.A. and Burger A.P. (1978). *A non-integrated, adiabatic three-level filtered weather prediction model.* CSIR Special Report, SWISK 7, Pretoria.
19. Riphagen H.A. (1984). *The implementation of a split explicit weather prediction model for the Southern Hemisphere.* M.Sc. dissertation, University of Pretoria, South Africa.
20. Riphagen H.A. and Burger A.P. (1986). Comments on the computational stability of Gadd's adjustment and advection schemes for a split explicit model. *Q. J. R. Met. Soc.* **112**, 276–282.
21. Riphagen H.A. and Van Heerden J. (1986). Comparative trials of a semi-Lagrangian advection scheme in a numerical weather prediction model. In *Proc. 12th South African Symposium on Numerical Mathematics, Umhlanga Rocks,* pp. 139–153.
22. Riphagen H.A. (1989). High latitude filtering for the global prediction model. In *Proc. 6th Annual Conference of the South African Society for Atmospheric Sciences, Pretoria,* p. 14.
23. Riphagen H.A. (1999). The Eta model in South Africa. *International Eta Model Newsletter,* No. 2, February 1999.
24. Riphagen H.A. (2000). Increased vertical resolution above elevated terrain in the Eta model through modification of the vertical coordinate. In *Proc. 16th Conference of the South African Society for Atmospheric Sciences, Pretoria,* p. P4.20.
25. Riphagen H.A., Bruyere C.L., Jordaan W., Poolman E.R. and Gertenbach J.D. (2002). Experiments with the NCEP regional Eta model at the South African Weather Bureau, with emphasis on terrain presentation and its effect on precipitation predictions. *Mon. Weath. Rev.* **130**, 1246–1263.
26. Tennant W.J., Riphagen H.A., Gertenbach J.D., De Villiers M.P. and Rae K.J. (1997). The effect of radiosonde and buoy reduction on numerical prediction products at the South African Weather Bureau. In *Proc. CGC/WMO Workshop on the Impact of Various Observing Systems on Numerical Weather Prediction, Geneva,* ed. J. Pailleux, World Weather Watch Technical Report No. 18, WMO/TD No. 868, 165–183.
27. Rautenbach C.J. deW. (1999). *Introduction of a hybrid vertical co-ordinate to an atmospheric general circulation model.* Ph.D. thesis, University of Pretoria, South Africa.
28. Burger A.P. (1991). The potential vorticity equation: from planetary to small scale. *Tellus* **43A**, 191–197.
29. Burger A.P. and Riphagen H.A. (1990). The basic equations in meteorological dynamics – a reexamination of unsimplified forms for a general vertical coordinate. *Beitr. Phys. Atmosph.* **63**, 151–164.
30. Burger A.P. and Riphagen H.A. (1999). Energy conservation for a general vertical coordinate – a reexamination of unsimplified forms. *Beitr. Phys. Atmosph.* **72**, 25–50.
31. White A.A., Hoskins B.J., Roulstone I. and Staniforth A. (2005). Consistent approximate models of the global atmosphere: shallow, deep, hydrostatic, quasi-hydrostatic and non-hydrostatic. *Q. J. R. Met. Soc.* **131**, 2081–2107.
32. Eckart C. (1960). *The Hydrodynamics of Oceans and Atmospheres.* Pergamon Press, Oxford.
33. White A.A. and Bromley R.A. (1995). Dynamically consistent, quasi-hydrostatic equations for global models with a complete representation of the Coriolis force. *Q. J. R. Met. Soc.* **121**, 399–418.
34. Dudhia J. and Bresch J.F. (2002). A global version of the PSU-NCAR mesoscale model. *Mon. Weath. Rev.* **130**, 2989–3007.
35. De Coning E. and Adam B.F. (2000). The tornadic thunderstorm events during the 1998–1999 South African summer. *Water SA* **26**, 361–376.
36. De Coning E., Adam B.F. and Banitz L. (2000). A severe weather event on 29 December 1997: synoptic and mesoscale perspectives. *Water SA* **26**, 137–146.
37. Landman W.A., Botes S., Goddard L. and Shongwe M.E. (2005). Assessing the predictability of extreme rainfall seasons over southern Africa. *Geophys. Res. Lett.* **32**, L23818, doi: 10.1029/2005GL023965.
38. Crimp S.J., Van den Heever S.C., D'Abreton P.C., Tyson P.D. and Mason S.J. (1997). *Mesoscale modelling of tropical-temperate troughs and associated systems over southern Africa.* WRC Report 595/1/97. Water Research Commission, Pretoria.
39. Crimp S.J., Lutjeharms J.R.E. and Mason S.J. (1998). Sensitivity of a tropical-temperate trough to sea-surface temperature anomalies in the Agulhas retroflection region. *Water SA* **24**, 93–100.
40. Joubert A.M., Katzfey J.J., McGregor J.L. and Nguyen K.C. (1999). Simulating mid-summer climate over southern Africa using a nested regional climate model. *J. Geophys. Res.* **104**, 19015–19025.
41. Tadross M.A., Jack C. and Hewitson B.C. (2006). On RCM-based projections of change in southern African summer climate. *Geophys. Res. Lett.* **32**, L23713, doi: 10.1029/2005GL024460.
42. Hansingo K. and Reason C.J.C. (2006). Sensitivity of the atmospheric response

to sea-surface temperature forcing in the South West Indian Ocean: a regional climate modelling study. *S. Afr. J. Sci.* **102**, 137–143.
43. Reason C.J.C. and Jagadheesha D. (2005). Relationships between South Atlantic SST variability and atmospheric circulation over the South African region during austral winter. *J. Climate* **18**, 3059–3075.
44. Singleton A.T. and Reason C.J.C. (2006). Numerical simulations of a severe rainfall event over the Eastern Cape coast of South Africa: sensitivity to sea surface temperature and topography. *Tellus* **58**A, 355–367.
45. Van Heerden J., Rautenbach C.J. deW. and Truter M.M. (1995). *Techniques for seasonal and longer term rainfall prediction in South Africa.* WRC Report 373/1/92. Water Research Commission, Pretoria.
46. Jury M.R., Pathack B., Rautenbach C.J. deW. and Van Heerden J. (1996). Drought over South Africa and Indian Ocean SST: statistical and GCM results. *Global Atmos. Ocean Syst.* **4**, 47–63.
47. Jury M.R., Mulenga H. and Rautenbach C.J. deW. (2000). Tropical Atlantic variability and Indo-Pacific ENSO: statistical analysis and numerical simulation. *Global Atmos. Ocean Syst.* **7**, 107–124.
48. Rautenbach C.J. deW. (2003). *Seasonal climate predictions with a coupled atmosphere–ocean general circulation model.* WRC Report 904/1/03. Water Research Commission, Pretoria.
49. Engelbrecht F.A., Rautenbach C.J. deW., McGregor J.L. and Katzfey J.J. (2002). January and July climate simulations over the SADC region using the limited-area model DARLAM. *Water SA,* **28**, 361–374.
50. Engelbrecht F.A. (2005). Simulations of climate and climate change over southern and tropical Africa with the conformal-cubic atmospheric model. In *Climate Change and Water Resources in Southern Africa*: *Studies on scenarios, impacts, vulnerabilities and adaptation,* ed. R.E. Schulze, chap. 4, pp. 57–74. WRC Report 1430/1/05. Water Research Commission, Pretoria.
51. Rautenbach C.J. deW., Engelbrecht F.A., Engelbrecht C.J., Ndarana T. and McGregor J.L. (2005). *Regional model development for simulating atmospheric behaviour and rainfall over southern Africa.* WRC Report 1261/1/05. Water Research Commission, Pretoria.
52. Engelbrecht F.A. (2006). *Theory and application of quasi-elastic equations in terrain-following coordinates based on the full pressure field.* Ph.D. thesis, University of Pretoria, South Africa.
53. White A.A. (1989). An extended version of a nonhydrostatic, pressure coordinate model. *Q. J. R. Met. Soc.* **115**, 1243–1251.
54. Miller M.J. and White A.A. (1984). On the nonhydrostatic equations in pressure and sigma coordinates. *Q. J. R. Met. Soc.* **110**, 515–533.
55. Haltiner G.J. and Williams R.T. (1980). *Numerical Prediction and Dynamic Meteorology,* 2nd edn. Wiley, New York.
56. Miller M.J. (1974). On the use of pressure as vertical coordinate in modelling convection. *Q. J. R. Met. Soc.* **100**, 155–162.
57. Laprise R. (1992). The Euler equations of motion with hydrostatic pressure as an independent variable. *Mon. Weath. Rev.* **122**, 3–26.
58. Juang H-M.H. (1992). A spectral fully compressible nonhydrostatic model in hydrostatic sigma coordinates: formulation and preliminary results. *Meteorol. Atmos. Phys.* **50**, 75–88.
59. Skamarock W.C., Klemp J.B., Dudhia J., Gill D.O., Barker D.M., Wang W. and Powers J.G. (2005). A description of the Advanced Research WRF Version 2. *NCAR Technical Note,* TN-468+STR.
60. Mesinger F. and Arakawa A. (1976). *Numerical Methods used in Atmospheric Models.* Vol. 1. GARP Publications Series No. 17.
61. McGregor J.L. (1993). Economical determination of departure points for semi-Lagrangian models. *Mon. Weath. Rev.* **121**, 221–230.
62. Shapiro R. (1975). Linear filtering. *Math. Comp.* **29**, 1094–1097.
63. Fischer G. (1965). On a finite difference scheme for solving the non-linear primitive equations for a barotropic fluid with application to the boundary current problem. *Tellus* **4**, 405–412.
64. Janjic Z.I. and Wiin-Nielsen A. (1977). On geostrophic adjustment and numerical procedures in a rotating fluid. *J. Atmos. Sci.* **34**, 297–310.
65. Straka J.M., Wilhelmson R.B., Wicker L.J., Anderson J.R. and Droegemeier K.K. (1993). Numerical solutions of a nonlinear density current: a benchmark solution and comparisons. *Int. J. Num. Methods Fluids* **17**, 1–22.
66. Wicker L.J. and Skamarock W.C. (2002). Time-splitting methods for elastic models using forward time schemes. *Mon. Weath. Rev.* **130**, 2088–2097.
67. Weisman M.L. and Klemp J.B. (1982). The dependence of numerically simulated convective storms on vertical wind shear and buoyancy. *Mon. Weath. Rev.* **110**, 504–520.
68. Thompson R.L., Edwards R., Hart J.A., Elmore K.L. and Markowski P. (2003). Close proximity soundings with supercell environments obtained from the Rapid Update Cycle. *Weath. Forecasting* **18**, 1243–1261.
69. Dupilka M.L. and Reuter G.W. (2006). Forecasting tornadic thunderstorm potential in Alberta using environmental sounding data. Part I: Wind shear and buoyancy. *Weath. Forecasting* **21**, 325–335.
70. Weisman M.L. and Klemp J.B. (1986). Characteristics of isolated storms. In *Mesoscale Meteorology and Forecasting,* ed. P.S. Ray, pp. 331–357. American Meteorological Society, Boston.
71. Fujita T. and Grandoso H. (1968). Split of a thunderstorm into anticyclonic and cyclonic storms and their motion as determined from numerical model experiments. *J. Atmos. Sci.* **35**, 1070–1096.
72. Klemp J.B. (1987). Dynamics of tornadic thunderstorms. *Annu. Rev. Fluid Mech.* **19**, 369–402.
73. Rotunno R. (1981). On the evolution of thunderstorm rotation. *Mon. Weath. Rev.* **109**, 171–180.
74. Davies-Jones R.P. (1983). The onset of rotation in thunderstorms. In *Preprints, 13th Conference of Severe Local Storms, Tulsa, Oklahoma,* 215–218. American Meteorological Society, Boston.